

Reduction of Cytochrome aa_3 Measured by Near-Infrared Spectroscopy Predicts Cerebral Energy Loss in Hypoxic Piglets

MILES TSUJI, HIROO NARUSE,¹ JOSEPH VOLPE, AND DAVID HOLTZMAN

Joint Program in Neonatology, Harvard Medical School [M.T.], and Department of Neurology, Children's Hospital and Harvard Medical School, Boston, Massachusetts 02115 [H.N., J.V., D.H.]

ABSTRACT

Near-infrared spectroscopy is a noninvasive monitoring technique that allows quantitative measurement of changes in cerebral oxygenated Hb (HbO_2), deoxygenated Hb (Hb), total Hb, and oxidized cytochrome aa_3 (CytO₂). Changes in cerebral Hb oxygenation and CytO₂ have been measured in human neonates and infants under a variety of conditions. However, the association of these measurements with cerebral high-energy phosphate loss is not known. We studied simultaneous changes in cerebral HbO_2 , Hb, total Hb, and CytO₂ by near-infrared spectroscopy and changes in nucleoside triphosphate (NTP, mostly ATP) and phosphocreatine (PC) concentrations and intracellular pH by *in vivo* ³¹P-labeled magnetic resonance spectroscopy. Four-wk-old piglets ($n = 8$) underwent sequential hypoxic episodes of increasing severity (inspired O₂ concentration, 12, 8, 6, 4, and 0%). Animals were anesthetized and mechanically ventilated. At all levels of hypoxia, cerebral HbO_2 decreased, and Hb increased. Loss of PC or NTP was not observed until inspired O₂ concentration was decreased to less than 12%. With such severe hypoxia, hypotension, intracellular acidosis, and increasingly severe PC and NTP depletions occurred. Decreases in PC and NTP correlated closely with decreased CytO₂ and arterial blood pressure ($p < 0.0001$) but not with changes in HbO_2 and Hb. In conclusion, cerebral hypoxemia is readily detected by near-

infrared spectroscopy as a decrease in HbO_2 and an increase in Hb. However, relative changes in cerebral HbO_2 and Hb have low predictive value for cerebral energy failure. Reduction of CytO₂ is highly correlated with decreased brain energy state and may indicate impending cellular injury. (*Pediatr Res* 37: 253–259, 1995)

Abbreviations

NIRS, near-infrared spectroscopy
 HbO_2 , oxygenated Hb
Hb, deoxygenated Hb
HbT, total Hb
CytO₂, oxidized cytochrome aa_3
PC, phosphocreatine
NTP, nucleoside triphosphate
Pi, inorganic phosphate
pHi, intracellular pH
MR, magnetic resonance
NMR, nuclear magnetic resonance
ABG, arterial blood gas
dpf, differential path-length factor
Pao₂, arterial Po₂
MAP, mean arterial pressure

Episodic or sustained hypoxemia and cerebral ischemia are frequent events in critically ill neonates and infants (1, 2). These conditions may contribute to brain injury through mechanisms that include a probable initial cellular energy failure (3–5). Detection of impending or early cellular energy failure may allow prevention of brain injury. Hence, recent interest in

neonatal cerebral monitoring has focused on noninvasive techniques to detect the presence of cerebral hypoxemia and ischemia.

NIRS is a light-based technique, which allows *in vivo* measurement of changes in cerebral HbO_2 , Hb, HbT (the sum of HbO_2 and Hb), and the level of CytO₂. Cytochrome aa_3 is the terminal enzyme of the mitochondrial electron transport chain, the site of electron transfer to molecular O₂. Because the NIRS technique is noninvasive and portable, it may provide a means to monitor cerebral oxygenation in human newborns and infants. Several investigators have demonstrated changes in NIRS measures of cerebral oxygenation in human neonates and infants during events such as apnea and bradycardia, suctioning, indomethacin treatment, and cardiopulmonary bypass (6–11). Typically, hypoxia is associated with decreased cerebral HbO_2 and increased Hb; CytO₂ does not change until hypoxia

Received May 13, 1994; accepted October 17, 1994.

Correspondence: Miles Tsuji, M.D., Joint Program in Neonatology, Brigham and Women's Hospital, CWN-4, 75 Francis St., Boston, MA 02115.

Supported by Cerebral Palsy Foundation Research Grant R-4010 (D.H.), National Institutes of Health Research Grant NS 26371 (D.H.), and a grant from the William Randolph Hearst Foundation (J.J.V.). M.T. was supported by National Institutes of Health Training Grant NS 07264 and Physician Scientist Award HD 01010. All experiments were performed at the Joint Center for Magnetic Resonance, Shields Warren Radiation laboratory, Boston, MA.

¹ Current address: Department of Obstetrics and Gynecology, Hamamatsu University School of Medicine, 2-12-12 Sumiyoshi, Hamamatsu, 430 Japan.

is marked. In humans, CytO₂ seems to be particularly responsive to changes in cerebral blood flow (6, 9, 12). However, the clinical and physiologic interpretations of these findings are uncertain. Because CytO₂ is an indicator of mitochondrial electron transport chain oxidation state, reduction of CytO₂ may be a specific indicator of inadequate cellular O₂ availability. However, correlations of CytO₂ signal with *in vivo* measures of brain cellular energy state have not been determined in these human studies.

In this study, cerebral Hb and mitochondrial oxygenation have been measured by NIRS, and cerebral PC, Pi, and NTP concentrations and pHi have been measured by ³¹P-labeled NMR spectroscopy in hypoxic piglets. These studies were designed to correlate the decreases in cerebral Hb oxygenation and CytO₂ with cerebral energy state using graded degrees of hypoxia.

METHODS

Animals. Four-wk-old miniature Yucatan piglets of both sexes were studied ($n = 8$; Charles River Laboratories, Wilmington, MA). Animals were obtained 1 d before study and allowed free access to food and water until the morning of the experiment. The studies were performed in compliance with institutional and National Institutes of Health guidelines for laboratory animal care (13).

For the experiments, the animals were anesthetized with chloral hydrate (400 mg/kg intraperitoneally, followed by 150 mg/kg/h by intraperitoneal infusion). After induction of anesthesia, animals were intubated and mechanically ventilated with a modified patient ventilator (model 3MV-PED, Emerson Co., Cambridge, MA). Temperature was maintained with a warming blanket at 36–38°C as measured with a rectal thermometer. Catheters were inserted through the surgically exposed right femoral artery and vein for arterial pressure monitoring and venous infusions. Catheters were continuously flushed at 2 mL/h with heparinized normal saline. ABG were measured in heparinized arterial blood samples with a commercial blood gas analyzer (model 280, Ciba Corning Diagnostics Corp., Medfield, MA). Ventilation was adjusted to maintain Pao₂ at 10.5–16.0 kPa, arterial Pco₂ at 4.5–6.0 kPa, and pH at 7.35–7.45 before the start of each hypoxic episode. In the normoxic periods, the inspired O₂ concentration was 25%.

For NIRS recordings, incisions were made in the scalp 1.5 cm on each side of the sagittal suture midway between the orbits and the external auditory meatus. Circular areas of scalp (approximately 1 cm in diameter) were removed, and acrylic plastic optode holders were attached to the skull with cyanoacrylate cement. The animal was then positioned supine on a specially constructed cradle with the head resting on a 4-cm-diameter MR surface coil. The anterior edge of the coil was positioned at a line between the orbits with the coil lying against the top of the skull. Fiber-optic bundles for conveying near-infrared light (NIRS optodes) were then attached to the optode holders and secured with plastic set screws with an interoptode space of 3.0–3.5 cm. The scalp under the MR

surface coil was left intact except where the optodes were attached to the skull.

After positioning in the magnet, animals were examined to ensure unconsciousness on the continuous chloral hydrate dose. Pancuronium (0.2 mg/kg bolus followed by 0.1 mg/kg/h i.v.) then was injected to decrease spontaneous respirations.

MR spectroscopy. ³¹P-labeled NMR spectra were acquired in the Fourier transform mode on a Bruker Biospec 4.7-tesla MR system. The surface coil positioned against the animal's skull was used in transmit and receive modes. The field homogeneity was optimized to 0.6 parts per million or less using the brain water signal. To sample more uniformly from the sensitive volume of the surface coil, an adiabatic half-passage stimulation pulse (hyperbolic secant) was used with a pulse width of 1 ms (14). Each spectrum was the average of 32 free-induction decay acquisitions with a recycle delay of 3 s. Each free induction decay consisted of 1024 data points and was zero filled to 2048 points for processing. The sweep width was 5000 Hz. Spectra were collected every 2 min before, during, and after hypoxic periods. Peak areas for Pi, PC, and β -NTP were determined by Lorentzian curve fitting and peak integration (MacFid software, Tecmag Co., Houston, TX). Changes in NTP concentration were assessed from the β -NTP peak, which shows little overlap with other metabolite peaks. The signal-to-noise ratio for the β -NTP peak was greater than 10. ATP represents at least 70% of the NTP signal (15, 16). Hence, acute changes in β -NTP imply changes in ATP. pHi was calculated from the chemical shift of the Pi peak relative to PC (17).

MR surface coils sample from an approximately hemispheric volume of one coil radius extending away from the coil (14). MR images of our piglets showed that the sample volume was confined primarily to the superior cerebral hemispheres (Fig. 1).

Near-infrared spectroscopy. The near-infrared spectrometer (NIRO-500, Hamamatsu Photonics K. K., Hamamatsu, Japan) used in this study produces light at four wavelengths (776, 828, 848, and 913 nm). Light at each frequency is transmitted in sequential pulses by a fiber-optic cable (optode) to the sample. Photons emerging from the sample are collected by the second

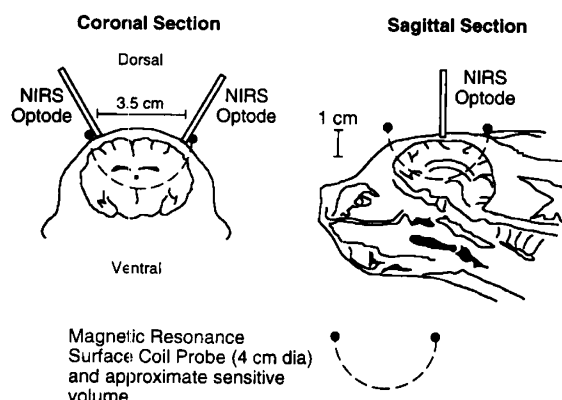


Figure 1. Coronal and sagittal diagrams of piglet head showing the MR coil and near-infrared optode positions. The surface coil is 4 cm in diameter and is shown with its approximate sensitive volume. These diagrams are derived from MR images of study animals.

optode and counted by a photomultiplier tube. The difference between transmitted and received light intensity at each wavelength was used to determine OD changes at each wavelength. Computer calculations based on chromophore absorption spectra then determined changes in HbO₂, Hb, and CytO₂ concentrations in micromoles per L times dpf according to the modified Beer-Lambert Law (18, 19). The dpf corrects the measured optode separation distance for light scattering within the sample. The measured dpf is 4.39 in human neonates and 4.34 in rats (18, 20–22). Because the dpf for piglet brain is not specifically known, results are expressed in concentration change times dpf. The dpf was assumed to be constant in each experiment. NIRS measurements were made with a sampling interval of 10 s. The HbT was calculated as the sum of HbO₂ plus Hb and used as a measure of cerebral blood volume.

The near-infrared light optodes were positioned over the cranium of each animal just inside the diameter of the MR surface coil. Although the brain volume sampled by the near infrared light is not precisely known, the spectrometer used in these experiments is capable of detecting Hb and CytO₂ signals in tissue with an optode separation of up to 6 cm. In addition, Monte Carlo mathematical modeling of photon travel in biologic scattering media suggests that NIRS used in these experiments should be sensitive to biologic signals from a circular arc with diameter of at least 80% of the interoptode space (Hamamatsu Photonics, unpublished data). Hence, it is likely that the near-infrared light penetrated throughout the sample radius of the MR surface coil (Fig. 1).

Protocol. To study the correlation of changes in HbO₂, Hb, and CytO₂ with PC and ATP depletion, animals were exposed to sequential brief episodes of increasingly severe hypoxia separated by recovery periods during which the animals breathed 25% O₂. After collection of baseline ³¹P-labeled NMR spectra and NIRS chromophore data, hypoxia was induced by changing the inspired O₂ concentration with a series of premixed O₂-N₂ cylinders (12%, 8%, 6%, and 4% O₂). Episodes of hypoxia were terminated with a return to 25% O₂ at 10 min or sooner (7 min) if severe bradycardia (heart rate, <80) occurred. Animals that survived all levels of hypoxia were studied while being killed by anoxia (100% N₂). ABG determinations were made just before and at the end of each hypoxemic episode. A repeat ABG measurement was made 15 min after each hypoxic episode, and bicarbonate (1–3 mEq/kg i.v.) was administered if necessary to correct metabolic acidosis. Recovery periods were approximately 30 min in duration,

as determined by normal blood gas parameters. NIRS data were recorded continuously. NMR spectra were acquired every 2 min before, during, and for 10 min after each episode of hypoxia.

Data analysis. Physiologic data before and after episodes of hypoxemia were compared by repeated-measures analysis of variance on the ranked data with the Scheffe technique for multiple comparisons. To eliminate the possible effect of small signal drifts during the entire course of the experiment, hypoxic chromophore values were compared with the prehypoxic values for each episode of hypoxia. The PC and NTP concentrations were similarly expressed as percent of the prehypoxic values for each hypoxic episode. There was no significant difference between PC and NTP levels before each episode of hypoxia. To simplify the data analysis and summarize the relationship between cerebral energy depletion and NIRS chromophore changes, the values for PC, NTP, and the chromophores HbO₂, Hb, and CytO₂ were compared at the end of each hypoxic episode, when these signals were maximally changed from baseline. For episodes in which the animals did not recover, the data values were assessed at 10 min after the onset of the hypoxia or anoxia. Comparisons of NMR and NIRS data at each level of hypoxia were made by analysis of variance on the ranked data as above. PC, NTP, and Pi values were then plotted against HbO₂, Hb, HbT, and CytO₂ and the relationships compared by calculating the Pearson correlation coefficients and Bonferroni corrected probability values. Because nonlinear relationships were observed between MAP and the other variables, these comparisons were made to Log-(MAP). *p* values < 0.05 were considered significant.

RESULTS

All eight animals survived the period in which they breathed 12 and 8% O₂. Three of eight animals died with 6% O₂ exposure, three of five died with 4% O₂ exposure, and the remaining two were killed with 0% O₂. The MAP and ABG values measured before the first hypoxic exposure and at the end of the hypoxic periods are summarized in Table 1. Progressively lower arterial Pao₂ values were seen with 12 and 8% inspired O₂ concentrations. No further decreases in Pao₂ were measured at lower O₂ exposures. Hyperventilation occurred despite pancuronium bromide treatment, as suggested by the lower arterial Pco₂ levels with severe hypoxia. Alternatively, hypoxia may have depressed cerebral metabolism and CO₂

Table 1. Blood gas values and MAP obtained before hypoxia (baseline) and at the end of each hypoxic period

O ₂ (%)	Pao ₂ (kPa)	Paco ₂ (kPa)	pH	MAP (kPa)
Baseline	14.71 ± 1.87	5.13 ± 0.45	7.37 ± 0.02	6.53 ± 2.04
12	5.65 ± 0.71	4.29 ± 0.73*	7.40 ± 0.06	7.45 ± 3.09
8	3.75 ± 0.65*†	4.31 ± 0.89*	7.40 ± 0.05	6.59 ± 3.28
6	3.57 ± 0.52*†	3.27 ± 0.60*†‡	7.43 ± 0.04*	2.87 ± 1.23
4	3.13 ± 0.44*†	2.56 ± 0.47*†‡	7.54 ± 0.06*†‡	1.56 ± 0.64*†‡
0	No result	No result	No result	0.44 ± 0.68*†‡

Values are mean ± SD.

* Different from baseline.

† Different from 12%.

‡ Different from 8%.

production. Arterial pH was unchanged, reflecting mixed respiratory alkalosis and metabolic acidosis, until the alkalemia seen with 4% inspired O₂. The MAP were unchanged with 12 and 8% O₂ exposures but decreased markedly with lower inspired O₂ exposures.

The NIRS tracing and NMR spectra from a typical experiment are shown in Figures 2 and 3. At each level of hypoxia, cerebral HbO₂ decreased, and Hb increased. Episodes of breathing less than 12% O₂ produced similar degrees of Hb deoxygenation. In the experiment shown, CytO₂ increased slightly at 12 and 8% O₂ exposures but decreased progressively with more severe decreases in inspired O₂. In Figure 3, the NMR spectra acquired before and immediately after each hypoxic episode are shown with the corresponding changes in CytO₂. The NMR spectra were unchanged with 12 and 8% inspired O₂. With episodes of more severe hypoxia, PC and NTP concentrations decreased, and Pi increased. Depletion of PC and NTP occurred during the episodes of hypoxia, which also produced reduction of CytO₂.

The temporal association of PC and NTP with changes in CytO₂ is shown in Figure 4. In this animal, moderate CytO₂ reduction and recovery occurred with 8% inspired O₂, and severe reduction without recovery occurred with 6% inspired O₂. The changes in PC were coincident with reduction in CytO₂. Changes in NTP lag the PC changes but were also temporally associated with CytO₂ reduction. HbO₂ and Hb reached their maximal changes before CytO₂, PC, and NTP changes.

The values at the end of each hypoxic exposure for all animals are summarized in Table 2. Cerebral HbO₂ decreased and Hb increased during all periods of hypoxia. Changes in HbT were variable. Slight increases in CytO₂ were seen with some 12 and 8% exposures (Figs. 3 and 4). However, this finding was not consistently present. Cerebral CytO₂ significantly and progressively decreased with inspired O₂ concentrations of 6% and lower. The onset of decreases in CytO₂ levels at 6% inspired O₂ and the progressive reduction of CytO₂ with more severe hypoxia were associated with the onset and the progression of decreases in MAP (Tables 1 and 2).

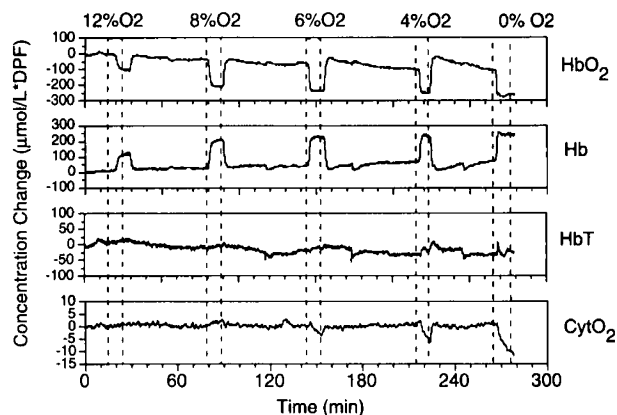


Figure 2. NIRS data from a 4-wk-old piglet exposed to increasingly severe episodes of hypoxia. The *x* axis is time in minutes. The *y* axes are concentration changes in $\mu\text{mol per L times dpf}$. Decrease in CytO₂ represents a reduction of cytochrome *aa*₃. Hypoxic episodes are shown in dotted outlines.

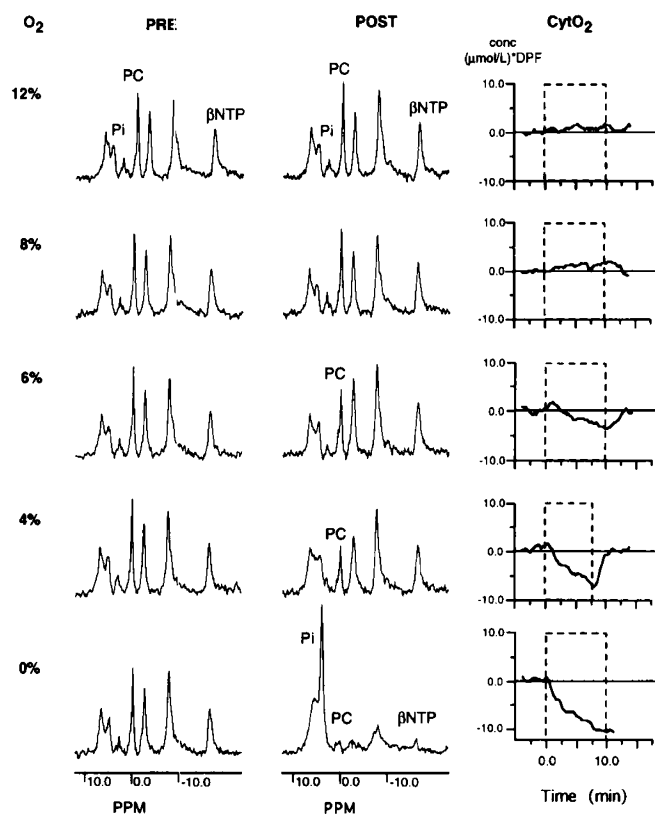


Figure 3. NMR data corresponding to the NIRS data shown in Figure 2. NMR spectra are plots of peak amplitude corresponding to amount of metabolite present vs resonant frequency that identifies the metabolites. The peaks for Pi, PC, and β -NTP (used to assess ATP level) are labeled. NMR spectra before and after each hypoxic episode (inspired O₂ concentrations of 12–0%) are shown with the corresponding changes in CytO₂ plotted as concentration change vs time in minutes. Depletion of PC first occurs with 6% O₂ exposure. In subsequent episodes, larger PC losses are seen, and NTP is also decreased. Episodes producing loss of PC and NTP are associated with CytO₂ decreases (reduction of cytochrome *aa*₃).

The NMR results are summarized in Table 3. With 12 and 8% inspired O₂, average PC and NTP decreases were small compared with baseline values measured before the first hypoxic episode. With more severe episodes of hypoxia, increasingly severe decreases in PC, NTP, and pH_i were observed in all animals. The declines in PC occurred earlier and were more marked than the declines in NTP. The decreases in PC and NTP at the 6% inspired O₂ concentration and the progressive reductions seen with more severe hypoxia were similar to the onset and progression of the decreases in CytO₂ and MAP (Tables 1–3).

Comparisons of the PC and NTP concentrations with NIRS measurements at the end of the hypoxic periods are shown in Figures 5 and 6. The changes in PC and NTP showed no correlations with HbO₂ or Hb (Fig. 5). In contrast, reduction of CytO₂ was closely correlated with decreases in PC and NTP and intracellular acidosis (Fig. 6). Losses of PC, NTP, and CytO₂ also were highly correlated with decreases in MAP in log-linear relationships.

DISCUSSION

The main findings of this study are a significant correlation of cerebral energy loss with CytO₂ reduction and a lack of

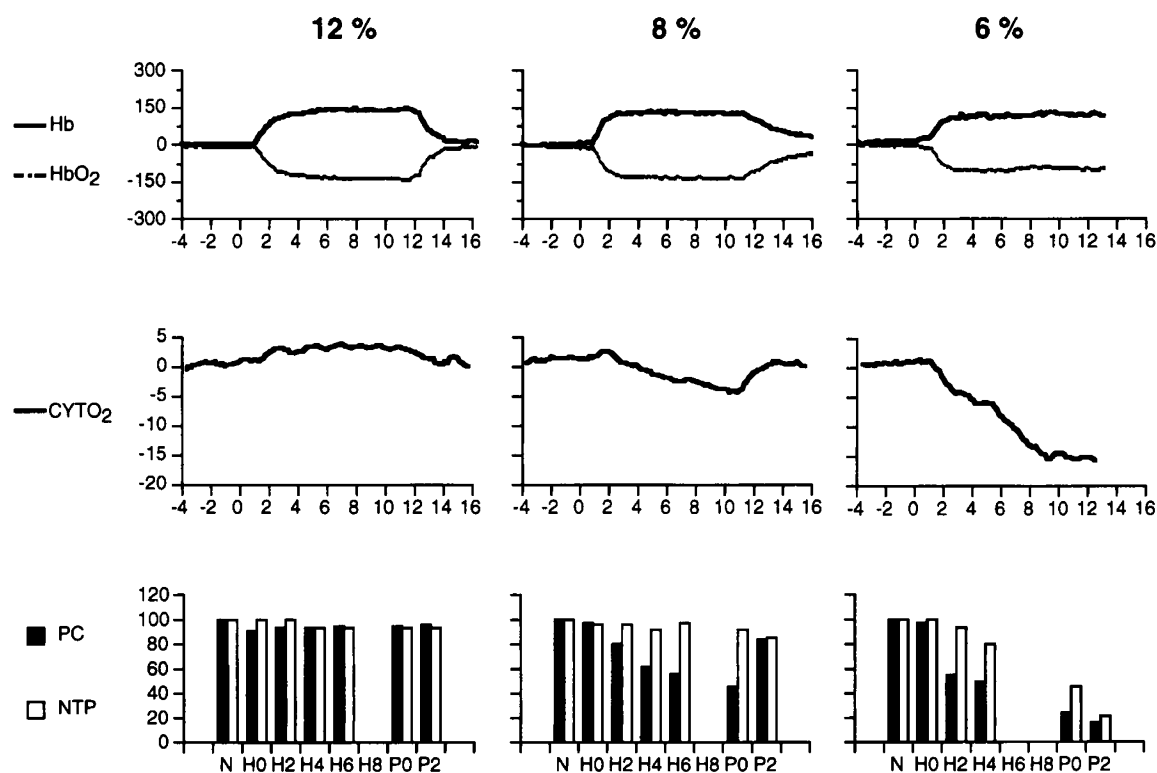


Figure 4. Temporal association of NIRS, NMR data in one piglet. The x axes are time in minutes. NMR data were shown for normoxic (N), hypoxic (H), and posthypoxic (P) conditions. Hypoxia starts at time 0 ($H0$) and extends to time 10 ($P0$). NIRS data are in $\mu\text{mol per L times dpf}$; NMR data are expressed as percent of baseline values. Decreases in CytO_2 temporally correspond to decreases in PC. More severe reduction of CytO_2 is accompanied by decreases in both PC and NTP. PC and NTP loss are not temporally associated with HbO_2 and Hb changes. NMR data are not available during arterial blood gas sampling at H8.

Table 2. Near-infrared spectroscopic measures of changes in HbO_2 and Hb, HbT, and CytO_2

O_2 (%)	HbO_2 [[$\mu\text{mol/L}$]:dpf]	Hb [[$\mu\text{mol/L}$]:dpf]	HbT [[$\mu\text{mol/L}$]:dpf]	CytO_2 [[$\mu\text{mol/L}$]:dpf]
12	-95.8 ± 31.6	113.2 ± 35.4	17.3 ± 9.3	0.1 ± 2.7
8	$-151.7 \pm 31.1^*$	182.6 ± 46.2	$30.9 \pm 19.6^\dagger$	-0.5 ± 4.6
6	$-167.0 \pm 53.1^*$	184.5 ± 61.4	17.5 ± 12.8	-5.1 ± 2.6
4	$-168.5 \pm 48.2^*$	165.7 ± 59.5	-2.8 ± 21.0	$-8.9 \pm 2.4^*\ddagger$
0	-208.2 ± 74.7	207.3 ± 62.7	-0.9 ± 12.0	$-14.1 \pm 1.0^*\ddagger\text{\S}$

Negative values indicated increased reduction. The values were taken from the spectra at the end of each hypoxic period. Values are mean \pm SD.

* Different from 12%.

† Different from 4%.

‡ Different from 8%.

§ Different from 6%.

correlation with cerebral Hb oxygenation. All levels of hypoxia produced decreases in HbO_2 and increases in Hb. Decreases in CytO_2 and depletion of PC and NTP were observed only in the more severe episodes of hypoxia, accompanied by systemic hypotension and probable cerebral ischemia.

The loss of PC and NTP with severe hypoxia and ischemia is in agreement with previous NMR studies in animals (23–26). As the primary energy metabolite of the cell, ATP is likely to be more sensitive to hypoxia and ischemia than other NTP that contribute to the NMR signal. Hence, the percent NTP losses observed in this study imply even larger fractional losses of ATP.

Our finding of cerebral energy metabolite loss with severe cerebral Hb deoxygenation also is consistent with previous observations that PC and NTP decline in the neonatal dog brain when inspired O_2 concentration and cerebral Hb saturation are

decreased to 10% or less (25, 27). However, in our study, such severe hypoxia produced both cerebral deoxygenation and systemic hypotension. Under these conditions, the magnitudes of HbO_2 and Hb did not correlate with PC and NTP levels.

Several mechanisms can explain the lack of correlation between cerebral energy loss and the degree of cerebral Hb deoxygenation. The presence of mixed hypoxia and ischemia may alter O_2 delivery greatly relative to hypoxia alone. In addition, cerebral energy metabolite levels are determined by the interaction of substrate and O_2 delivery, energy production pathways, and energy use. Hence, numerous observers have suggested that a specific "critical PaO_2 " for cerebral energy failure does not exist (28, 29). NIRS measures global cerebral HbO_2 and Hb levels. However, changes in the relative sizes of the arterial and venous compartments in the cerebral circulation and decreased rates of tissue O_2 consumption could result

Table 3. Changes in concentrations of PC, NTP, Pi, and pHi derived from ^{31}P NMR spectra

%O ₂	PC (%)	NTP (%)	Pi (%)	pHi
12	101 ± 7	99 ± 5	118 ± 18	7.24 ± 0.13
8	91 ± 19	98 ± 5	93 ± 15	7.15 ± 0.15
6	52 ± 23*†‡	83 ± 18*	157 ± 105	6.89 ± 0.18*†‡
4	29 ± 22*†‡	60 ± 30*†‡	254 ± 217	6.62 ± 0.11*†‡
0	28 ± 15*†	47 ± 29*†‡	229 ± 120	6.47 ± 0.21*†‡

NTP levels are assumed to reflect changes in ATP concentration, which accounts for the majority of the NTP signal and is the NTP most sensitive to hypoxia. Except for pHi, all values are expressed as percent of prehypoxic values. The prehypoxic pHi was 7.10 ± 0.10 . The hypoxemic values are taken from spectra acquired at the end of each hypoxic period or after 10 min of breathing N₂. Values are mean ± SD.

* Different from baseline.

† Different from 12%.

‡ Different from 8%.

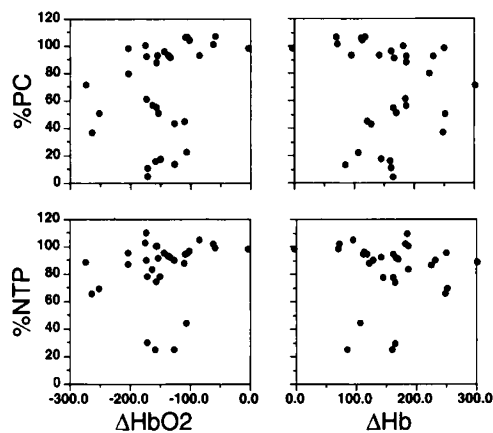


Figure 5. Plots showing PC and NTP losses vs HbO₂ and Hb. Each point is the change observed at the end of one hypoxic episode in one animal. PC and NTP are expressed as the percent of their prehypoxic values. Changes in NTP are reflective of changes in ATP (see Table 3). HbO₂ and Hb are expressed in $\mu\text{mol per L times dpf}$. HbO₂ always decreases and Hb always increases with hypoxia, but the magnitudes of the changes are poorly correlated with cellular energy loss. Correlation coefficients: PC vs HbO₂, 0.47, NS; PC vs Hb, -0.34, NS; NTP vs HbO₂, -0.34, NS; NTP vs Hb, -0.22, NS.

in similar HbO₂ and Hb levels for widely differing levels of O₂ delivery and cellular oxygenation. In our study, hypoxia produced varying degrees of cardiac compromise and hyperventilation in the piglet. The HbT changes were small and inconsistent, even when MAP fell, suggesting that hypoxic cardiac failure may have produced both decreased arterial flow and venous congestion. In both clinical and animal hypoxia, associated systemic and cerebral hemodynamic changes are likely. Hence, the interactions of variables affecting cerebral Hb oxygenation are complex, and the relationships between cerebral Hb oxygenation and brain cellular oxidation-reduction state and energy levels are not direct.

In our study, cerebral ischemia may be causally related to both the decreased CytO₂ and loss of high-energy phosphate compounds. Both CytO₂ and the PC and NTP concentrations decreased in parallel with decreases in MAP. Because hypoxemia can impair cerebrovascular autoregulation (4, 29, 30), the onset and the progression of the decreases in MAP at the inspired O₂ concentrations less than 8% probably were accompanied by progressive decreases in cerebral blood flow and significant decreases in O₂ delivery. This decrease in cerebral blood flow may have been accentuated by the decreases in P_{aco}₂ with inspired O₂ concentrations less than 8% (30, 31). The declines in CytO₂ and in PC and NTP concentrations,

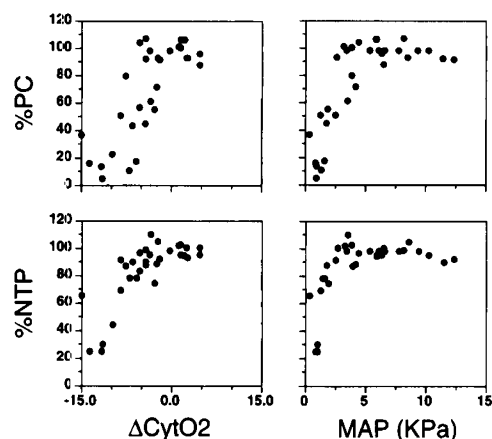


Figure 6. Plots showing PC and NTP loss vs CytO₂ and MAP. Each point is the change observed at the end of one hypoxic episode in one animal. PC and NTP are expressed as the percent of their prehypoxic values. Changes in NTP are reflective of changes in ATP (see Table 3). CytO₂ is expressed in $\mu\text{mol per L times dpf}$. MAP is expressed in kPa. A significant correlation is shown between the energy metabolites PC, NTP, and changes in CytO₂ and MAP less than 5 kPa. Correlation coefficients: PC vs CytO₂, 0.79, $p < 0.001$; PC vs Log(MAP), 0.79, $p < 0.001$; NTP vs CytO₂, 0.77, $p < 0.001$; NTP vs Log(MAP), 0.63, $p < 0.005$; CytO₂ vs Log(MAP), 0.65, $p < 0.001$; CytO₂ vs pHi, 0.68, $p < 0.001$ (not shown).

which correlated well with these decreases in MAP, are consistent with extensive *in situ* and *in vitro* studies of cerebral blood flow and cellular energetics in the animal brain (4, 32). The particular sensitivity of CytO₂ to cerebral perfusion also is suggested by studies in human infants showing declines in CytO₂ under conditions known to cause diminished cerebral blood flow *i.e.* hypocarbia and indomethacin infusion (9, 12).

The accuracy and specificity of bedside measurement of cytochrome *aa*₃ redox changes by NIRS are not definitively established (33). Interpretation of the CytO₂ signal is further complicated by differences in the instrumentation and algorithms used to derive the CytO₂ signal (20, 33–35). The correlation between PC levels and CytO₂ has been previously suggested from changes in light absorption at 780–830 nm (36). However, that technique did not directly exclude the effect of absorption by blood Hb. Our study used four near-infrared wavelengths and algorithms previously used in human studies (12, 18, 20). Hence, the observed correlations are more comparable with previous human data. The correlation between ATP and CytO₂ supports the interpretation that the CytO₂ signal closely reflects, if not directly measures, brain cellular oxidation-reduction state.

The observed correlation between decreases in CytO₂ and decreased NTP and PC concentrations in the cerebral cortex will be of great clinical use. In conditions such as respiratory or cardiac failure, cardiopulmonary bypass, extracorporeal membrane oxygenation, and increased intracranial pressure, the NIRS CytO₂ signal may be a better predictor of cellular energy state in brain than commonly used clinical measurements such as arterial O₂ saturation and Pao₂. As a portable system, NIRS now is being applied in monitoring the brain in critically ill newborns and young infants (8, 9, 11). The significance of decreases in CytO₂ in these studies has been unclear. Our results strongly suggest that such decreases indicate cerebral energy loss and, hypothetically, an increased risk of brain injury.

Further studies combining NIRS with NMR and other physiologic measures, such as cerebral blood flow, tissue O₂ concentration, and electroencephalography are necessary. Cerebral energy metabolism is known to vary with maturation, temperature, and metabolic stress (27, 37–39). It is possible that the relative coupling between CytO₂ and cerebral energy metabolite levels could be affected by these parameters. In this study, we examined 4-wk-old piglets, which may be comparable with slightly younger human neonates (40–42). Further studies will be required to define maturational patterns. The observation that CytO₂ levels increased during 12 or 8% hypoxic exposure in some of our study animals also awaits further study. If this finding is confirmed, it may indicate that CytO₂ can increase under certain conditions of metabolic stress. An understanding of the *in situ* physiology of brain cellular ATP regulation and maintenance of cellular viability under conditions of metabolic stress will be critical in developing NIRS as a clinical monitoring technique.

Acknowledgments. The authors thank Colin Cook, Ron Meyer, Trinh Quach, Steven Telio, and Ann Celi for technical assistance.

REFERENCES

- Volpe JJ 1989 Current concepts of brain injury in the premature infant. *AJR Am J Roentgenol* 153:243–251
- Volpe JJ 1994 Hypoxic-ischemic encephalopathy biochemical and physiological aspects. In: *Neurology of the Newborn*, 3rd Ed. WB Saunders, Philadelphia, pp 160–189
- Auer RN, Siesjo BK 1988 Biological differences between ischemia, hypoglycemia, and epilepsy. *Ann Neurol* 24:699–707
- Raichle ME 1983 The pathophysiology of brain ischemia. *Ann Neurol* 13:2–10
- Vannucci RC 1990 Experimental biology of cerebral hypoxia-ischemia: relation to perinatal brain damage. *Pediatr Res* 27:317–326
- Greeley WJ, Bracey VA, Ungerleider RM, Greibel JA, Kern FH, Boyd JL, Reves JG, Piantadosi CA 1991 Recovery of cerebral metabolism and mitochondrial oxidation state is delayed after hyperthermic circulatory arrest. *Circulation* 84:III400–III406
- Reynolds EO, Wyatt JS, Azzopardi D, Delpy DT, Cady EB, Cope M, Wray S 1988 New non-invasive methods for assessing brain oxygenation and haemodynamics. *Br Med Bull* 44:1052–1075
- Livera LN, Spencer SA, Thorniley MS, Wickramasinghe YABD, Rolfe P 1991 Effects of hypoxaemia and bradycardia on neonatal cerebral haemodynamics. *Arch Dis Child* 66:376–380
- Edwards AD, Wyatt JS, Richardson C, Potter A, Cope M, Delpy DT, Reynolds EO 1990 Effects of indomethacin on cerebral haemodynamics in very preterm infants. *Lancet* 335:1491–1495
- Brazy JE, Lewis DV 1986 Changes in cerebral blood volume and cytochrome *aa*₃ during hypertensive peaks in preterm infants. *J Pediatr* 108:983–987
- Shah AR, Kurth CD, Gwiazdowski SG, Chance B, Delivoria-Papadopoulos M 1992 Fluctuations in cerebral oxygenation and blood volume during endotracheal suctioning in preterm infants. *J Pediatr* 120:769–774
- Edwards AD, Brown GC, Cope M, Wyatt JS, McCormick DC, Roth SC, Delpy DT, Reynolds EO 1991 Quantification of concentration changes in neonatal human cerebral oxidized cytochrome oxidase. *J Appl Physiol* 71:1907–1913
- National Academy of Science 1985 *Guide for the Care and Use of Laboratory Animals*, NIH Pub 86. National Institutes of Health, Bethesda, MD, pp 1–23
- Bendall MR 1990 Theory and technique of surface coils in *in vivo* spectroscopy. In: Pettegrew J (ed) *NMR: Principles and Applications to Biomedical Research*. Springer-Verlag, New York, pp 401–428
- Chapman A, Westerber E, Siesjo B 1981 The metabolism of purine and pyrimidine nucleotides during insulin-induced hypoglycemia and recovery. *J Neurochem* 36:179–189
- Lolley R, Balfour W, Samson F 1961 The high energy phosphates in developing brain. *J Neurochem* 7:289–297
- Petroff OA, Prichard JW, Behar KL, Alger JR, den Hollander JA, Shulman RG 1985 Cerebral intracellular pH by 31P nuclear magnetic resonance spectroscopy. *Neurology* 35:781–788
- Wyatt JS, Cope M, Delpy DT, Wray S, Reynolds EO 1986 Quantification of cerebral oxygenation and haemodynamics in sick newborn infants by near infrared spectrophotometry. *Lancet* 2:1063–1066
- Van der Zee P, Delpy DT 1988 Methods of quantitating cerebral near infrared spectroscopy data. *Adv Exp Med Biol* 222:183–189
- Wray S, Cope M, Delpy DT, Wyatt JS, Reynolds EO 1988 Characterization of the near infrared absorption spectra of cytochrome *aa*₃ and haemoglobin for the non-invasive monitoring of cerebral oxygenation. *Biochim Biophys Acta* 933:184–192
- Delpy DT, Arridge SR, Cope M, Edwards D, Reynolds EO, Richardson CE, Wray S, Wyatt J, van der Zee P 1990 The effect of optode positioning on optical path length in near infrared spectroscopy of brain. *Adv Exp Med Biol* 277:79–84
- Cope M, Delpy DT, Wray S, Wyatt JS, Reynolds EO 1989 Quantitation of pathlength in optical spectroscopy. *Adv Exp Med Biol* 248:41–46
- Hope PL, Cady EB, Chu A, Delpy DT, Gardiner RM, Reynolds EO 1987 Brain metabolism and intracellular pH during ischaemia and hypoxia: an *in vivo* 31P and 1H nuclear magnetic resonance study in lamb. *J Neurochem* 49:75–82
- Jensen F, Tsuji M, Ofutt M, Firkusny I, Holtzman D 1993 Profound reversible energy loss in the hypoxic immature brain. *Dev Brain Res* 73:99–105
- Nioka S, Smith DS, Chance B, Subramanian HV, Butler S, Katzenberg M 1990 Oxidative phosphorylation system during steady-state hypoxia in the dog brain. *J Appl Physiol* 68:2527–2535
- Gyulai L, Schnall M, McLaughlin AC, Leigh JS, Chance B 1987 Simultaneous ³¹P and ¹H-nuclear magnetic resonance studies of hypoxia and ischemia in the cat brain. *J Cereb Blood Flow Metab* 7:543–551
- Nioka S, Chance B, Smith DS, Mayevsky A, Reilly MP, Alter C, Asakura T 1990 Cerebral energy metabolism and oxygen state during hypoxia in neonate and adult dogs. *Pediatr Res* 28:54–62
- Rosenthal M, Lamanna JC, Jobsis FF, Levasseur JE, Kontos HA, Patterson JL 1976 Effects of respiratory gases on cytochrome A in intact cerebral cortex: is there a critical P_{o2}? *Brain Res* 108:143–154
- Siesjo B 1978 Hypoxia. In: *Brain Energy Metabolism*. Wiley, Chichester, UK, pp 411–422
- Hansen NB, Brubakk A, Bratlid D, Oh W, Stonestreet BS 1984 The effects of variations of P_{aCO2} on brain blood flow and cardiac output in the newborn piglet. *Pediatr Res* 18:1132–1136
- Pryds O, Greisen L, Skov L, Friis-Hansen B 1990 Carbon dioxide-related changes in cerebral blood volume and cerebral blood flow in mechanically ventilated preterm neonates: comparison of near infrared spectrophotometry and 133-xenon clearance. *Pediatr Res* 27:445–449
- Siesjo BK 1988 Mechanisms of ischemic brain damage. *Crit Care Med* 16:954–963
- Hirtz DG 1993 Report of the national institute of neurological disorders and stroke workshop on near infrared spectroscopy. *Pediatrics* 91:414–417
- Benaron DA, Benitz WE, Ariagno RL, Stevenson DK 1992 Noninvasive methods for estimating in-vivo oxygenation. *Clin Pediatr (Phila)* 31:258–273
- Vanderkooij JM, Erecinska M, Silver IA 1991 Oxygen in mammalian tissue: methods of measurement and affinities of various reactions. *Cell Physiol* 29:C1131–C1150
- Tamura M, Hazeki O, Nioka S, Chance B, Smith DS 1988 The simultaneous measurements of tissue oxygen concentration and energy state by near-infrared and nuclear magnetic resonance spectroscopy. *Adv Exp Med Biol* 222:359–363
- Busto R, Dietrich W, Globus M, Valdes I, Scheinberg P, Ginsberg M 1987 Small differences in intracerebral brain temperature critically determine the extent of ischemic neuronal injury. *J Cereb Blood Flow Metabol* 7:729–738
- Chugani HT, Phelps ME 1986 Maturational changes in cerebral function in infants determined by 18FDG positron emission tomography. *Science* 231:840–843
- Duckrow RB, LaManna JS, Rosenthal M 1981 Disparate recovery of resting and stimulated oxidative metabolism following transient ischemia. *Stroke* 12:677–686
- Raju TNK 1992 Some animal models for the study of perinatal asphyxia. *Biol Neonate* 62:202–214
- Laptook A, Stonestreet BS, Oh W 1982 The effects of different rates of plasmanate infusions upon brain blood flow after asphyxia and hypotension in newborn piglets. *J Pediatr* 100:791–796
- Dickerson JWT, Dobbing J 1967 Prenatal and postnatal growth and development of the central nervous system of the pig. *Proc R Soc Lond [Biol]* 166:384–395